Electron beam stimulated formation of CdS nanoparticles within calixarene Langmuir–Blodgett films

A. V. Nabok, A. K. Ray, and A. K. Hassan
*Fibre-Optics & Physical Electronics Research Laboratories, Electronic Research Group,
School of Engineering, Sheffield Hallam University, City Campus Pond Street,
Sheffield S1 1WB, United Kingdom*

Two possible types of cadmium sulphide (CdS) nanostructures can be formed within Langmuir–Blodgett (LB) films of calixarene Cd salt as a result of exposure to H_2S gas: nanoclusters with the size of about 1.5 nm or two-dimensional planes with the thickness of about 1.7 nm. Transmission electron microscopy and electron diffraction studies on calixarene/CdS LB films show that CdS particles are not present in the fresh samples at the beginning, but they are gradually formed under exposure to a high energy electron beam. A blueshift of the first exciton absorption band and an increase of the extinction coefficient, caused by exposure to H_2S gas, were found with UV-visible optical spectroscopy and surface plasmon resonance, respectively. © *2000 American Institute of Physics.* [S0021-8979(00)07015-8]

I. INTRODUCTION

The main trend of microelectronics toward decreasing the feature size stimulates great interest in the development of nanoelectronic devices such as: resonance tunneling devices based on III–V semiconductor superlattices,[1] silicon quantum dots,[2] and single-electron tunneling transistors.[3,4] The formation of nanosized elements requires some sophisticated and expensive technologies such as, molecular beam epitaxy (MBE), advanced x-ray and electron-beam lithography, scanning probe techniques, such as STM and AFM, etc., employing ultrahigh vacuum equipment and super clean environmental conditions. Alternatively, the wet technology has been adapted for producing nanosized elements due to recent achievements of colloid and organic chemistry and technology of thin organic films.[5] A variety of colloid nanoparticles including metals (Au, Ag, Pt, Pd), semiconductors (CdS, CuS, CdSe, PbSe, PbTe, TiO_2), and insulators (ceramic, mica) have now become commercially available.[5] These particles can be chemically modified and deposited by different techniques, such as Langmuir–Blodgett (LB)[6] and polyelectrolyte self-assembly methods.[7,8]

A simple but elegant method of formation of II–VI semiconductor nanoparticles within LB film matrix has been proposed earlier by Barraud and co-workers[9,10] with a view to forming two-dimensional (2D) semiconductor layers. By exposing LB films of fatty acid metal salt (cadmium stearate, for example) to H_2S gas, metal sulphide (CdS) can be formed due to the following reaction:

$$(CH_3-(CH_2)_n-COO)_2Cd+H_2S$$
$$=2(CH_3-(CH_2)_n-COOH)+CdS.$$
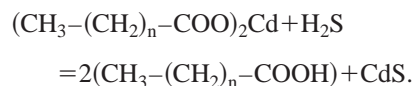
It was found that clusters of metal sulphides (CdS, PbS, CuS) with the size of 3–5 nm were formed within the fatty acid LB film matrix due to molecular segregation.[10–14] A similar idea has been exploited in our previous publications[15–17] to form CdS nanoparticles within calixarene LB films. It was suggested there that the presence of calixarene cavities restricts segregation of CdS, and much smaller CdS particles were formed as a result. The size of 1.5 ± 0.3 nm for CdS particles embedded into calixarene LB films was estimated from their UV-visible absorption spectra.[15,16] However, both low angle x-ray diffraction[16] and AFM[17] experiments showed no respective changes in the diffraction pattern and morphology of calixarene LB films after exposure to H_2S gas. Transmission electron microscopy (TEM) showed no CdS particles on fresh samples during initial stages of inspection, but they grew later, possibly, stimulated by the electron beam.[17]

In the present work the formation of CdS nanoparticles in calixarene LB films was studied *in situ* using TEM and electron diffraction. Additional UV-visible optical spectroscopy and surface plasmon resonance (SPR) measurements were performed here in order to register changes of the optical parameters of calixarene LB films caused by the formation of CdS nanostructures. Possible applications are highlighted.

II. EXPERIMENTAL DETAILS

Tert-octyl calix[8]arene carboxylic acid, referred throughout the text as C[8]A (see chemical structures in Fig. 1) was chosen for LB film deposition. 0.5 mg/ml solution of C[8]A compound in chloroform was spread onto Millipore water subphase containing 5×10^{-4} M $CdCl_2$ in order to form Cd salts in monolayers. The films were then transferred onto hydrophobic substrates at a constant surface pressure of 25 mN/m and at a deposition speed of 5 mm/min for both down and up strokes. UV-visible absorption spectra of LB films transferred onto quartz slides were measured at room temperature on the same samples before and after H_2S treatment by using a UV4 UNICAM spectrophotometer. The spectra of CdS embedded into the film were then obtained by subtraction of the spectra measured before and after exposure
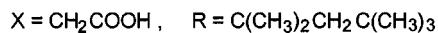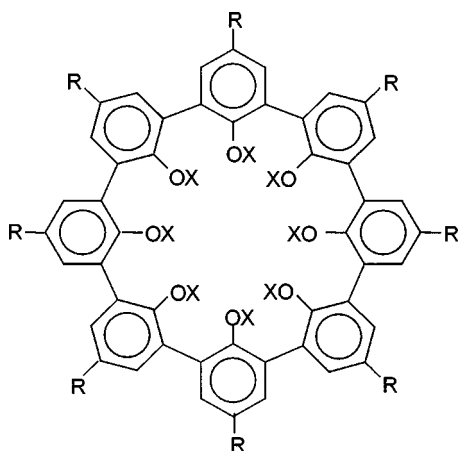
1333

$X = CH_2COOH$, $R = C(CH_3)_2CH_2C(CH_3)_3$

FIG. 1. Chemical structures of calix[8]arene acid.

FIG. 3. A schematic model of 2D CdS planes within calixarene LB film: the thickness of the C[8]A bilayer is 3 nm; the thickness of the CdS layer is 1.7 nm.

to H_2S. Procedures of C[8]A LB film deposition, treatment of the samples with H_2S, and optical characterization have been described in detail earlier.[15]

TEM and electron diffraction studies were performed on LB films deposited onto 300 mesh copper grids coated with amorphous carbon (Agar Scientific, UK). These measurements were performed using a Philips CM20 TEM operating at 200 keV (electron wavelength of 0.002 51 nm). Electron diffraction patterns were recorded using an unfocused electron beam of about 0.5 μm in diameter. In order to study the effect of the dose of electron irradiation, series of TEM pictures and diffraction patterns were taken at an interval of 5 min from the film exposure under the focused electron beam.

SPR measurements were carried out on C[8]A LB films transferred onto the 45 nm gold coated glass slides, using a Kretschmann type θ–2θ rotated stage experimental setup described previously.[18] The samples were brought into optical contact with the semicylindrical prism using index-matching liquid. A p-polarized HeNe laser source ($\lambda = 632.8$ nm) was used for the excitation of surface plasmons. The SPR curves
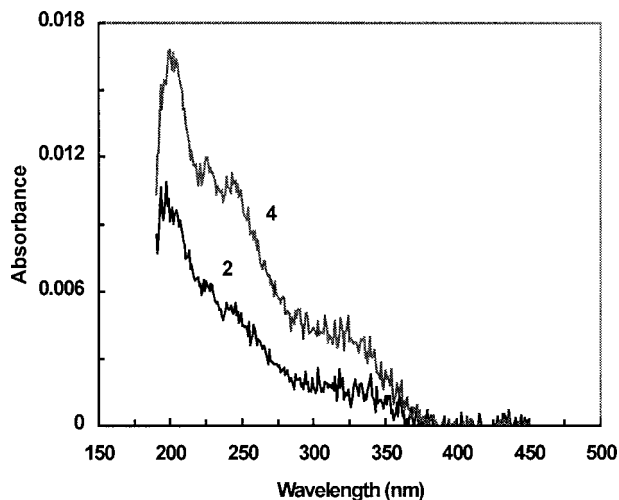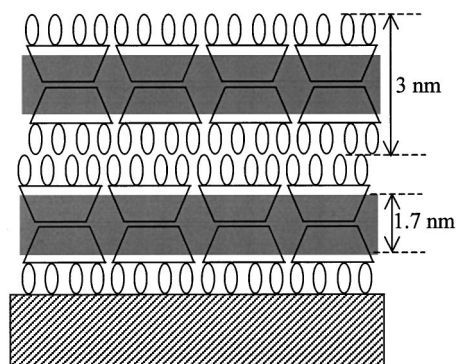
were measured on the same samples before and after exposure to H_2S gas. Thickness d, refractive index n, and extinction coefficient k of calixarene thin films were evaluated by fitting the experimental SPR curves to Fresnel's theory using a least-square technique.[18,19]

III. RESULTS AND DISCUSSION

Typical UV-visible absorption spectra of CdS imbedded into C[8]A LB films (two and four layers) are shown in Fig. 2. The absorption edge at 370 nm corresponds to the energy of 3.35 eV, which is much higher than that for bulk CdS (2.4 eV). The observed blueshift of the absorption edge is believed to be caused by size quantization of exitons in CdS clusters.[20] The size of semiconductor nanoclusters can be estimated from the method due to Ramakrishna[21] based on direct calculations of the band structure of semiconductors using the method of pseudopotential. The size effect is investigated using the following expression for exciton energy in CdS spherical clusters with the radius R:[22,23]
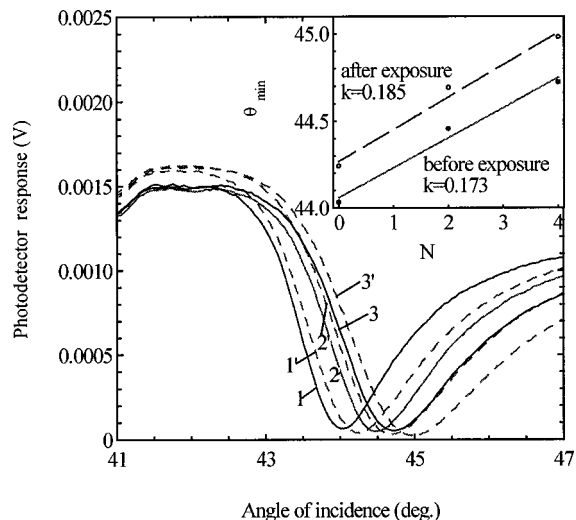
FIG. 2. UV-vis absorption spectra of CdS embedded into C[8]A LB films. Number of layers are shown next to respective curve.

FIG. 4. Experimental SPR curves for 45 nm gold layer (1, 1′) coated with C[8]A LB films of two layers (2, 2′) and four layers (3, 3′). Dashed line corresponds to SPR curves after exposure to H_2S gas. The inset shows dependencies of the position of the minimum of SPR curves on the number of LB layers.

TABLE I. Optical parameters obtained by SPR fitting for bare gold and LB films.

	Bare gold layer			Two LB layers of C[4]A			Four LB layers of C[4]A		
	n	k	d (nm)	n	k	d (nm)	n	k	d (nm)
Before H$_2$S	0.188	3.337	45.03	1.46	0	1.58	1.46	0	3.09
After H$_2$S	0.279	3.248	47.28	1.47	0.244	1.58	1.45	0.115	3.09

$$E = E_g - \frac{1.786 e^2}{\varepsilon R} - 0.248 E_R, \quad (1)$$

where E_g is the band gap of the bulk material, and ε is the dielectric constant of CdS. The second term in Eq. (1) represents Coulomb interaction between electrons and holes. The exciton binding energy is given in the form

$$E_R = \frac{\mu e^2}{2\varepsilon^2 \hbar^2}, \quad (2)$$

where μ is the exciton reduced mass

$$\left(\frac{1}{\mu} = \frac{1}{m_e^*} + \frac{1}{m_h^*} \right).$$

Using the $E(R)$ diagram from Ref. 21 a value of 1.5 nm was found for the diameter of CdS clusters embedded into C[8]A LB film. This value is much smaller than 3–5 nm usually observed for CdS nanoparticles in fatty acid LB films.[11–15] This leads to an inference that calixarene cavities limit the segregation of CdS particles within the film.

It can also be argued that CdS forms two-dimensional planes within each bilayer of calixarene LB films. In this case, energy spectra $E_{e,h}$ of electrons and holes within a layer of thickness L_Z will be described as follows:[24]

$$E_{e,h} = \frac{\hbar^2 (k_X^2 + k_Y^2)}{2 m_{e,h}^*} + \frac{\hbar^2 \pi^2}{2 m_{e,h}^*} \frac{n_z^2}{L_Z^2}. \quad (3)$$

Here the first term describes the motion of electrons and holes with the respective effective mass m_e^* or m_h^* within the x,y plane, while the second term shows the series of levels of size quantization in the z direction with the principal quantum number n_Z. The first exciton band in this case can be described as[20]

$$E = E_g - E_{\text{ex}}^{2D} + \frac{\pi^2 \hbar^2}{2\mu L_Z^2}, \quad (4)$$

where $E_g = 2.425$ eV is the band gap for bulk CdS at room temperature, E_{ex}^{2D} is 2D exciton binding energy, which is four times larger than $E_{\text{ex}} = 0.028$ eV for bulk CdS,[20] and $\mu = 0.125 m_0$. A value of 1.7 nm is obtained for L_Z, which is almost twice the cavity depth of calixarene. The formation of CdS planes can be postulated within each calixarene bilayer (see a scheme in Fig. 3), capturing CdS molecules in calixarene intrinsic cavities and, possibly, in the free space between molecules. This model is consistent with an earlier
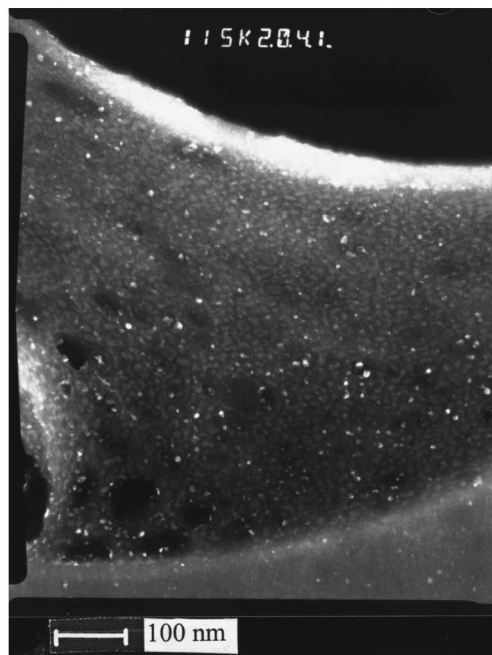
(a)
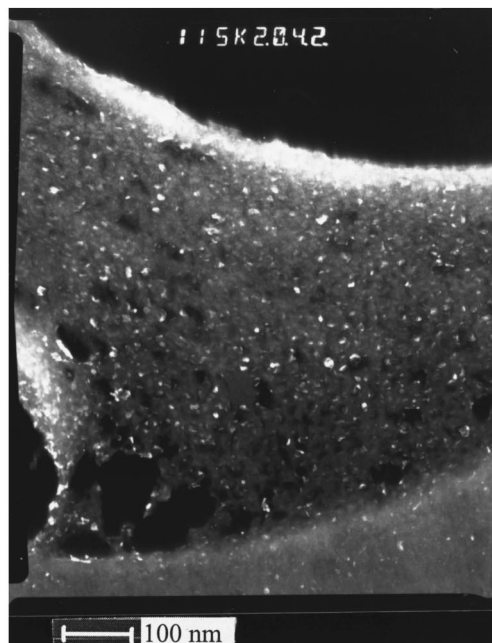
(b)

FIG. 5. TEM images of C[8]A LB film (ten layers) exposed to H$_2$S gas. Magnification is of 115 000. Photo (b) is taken 5 min after (a).
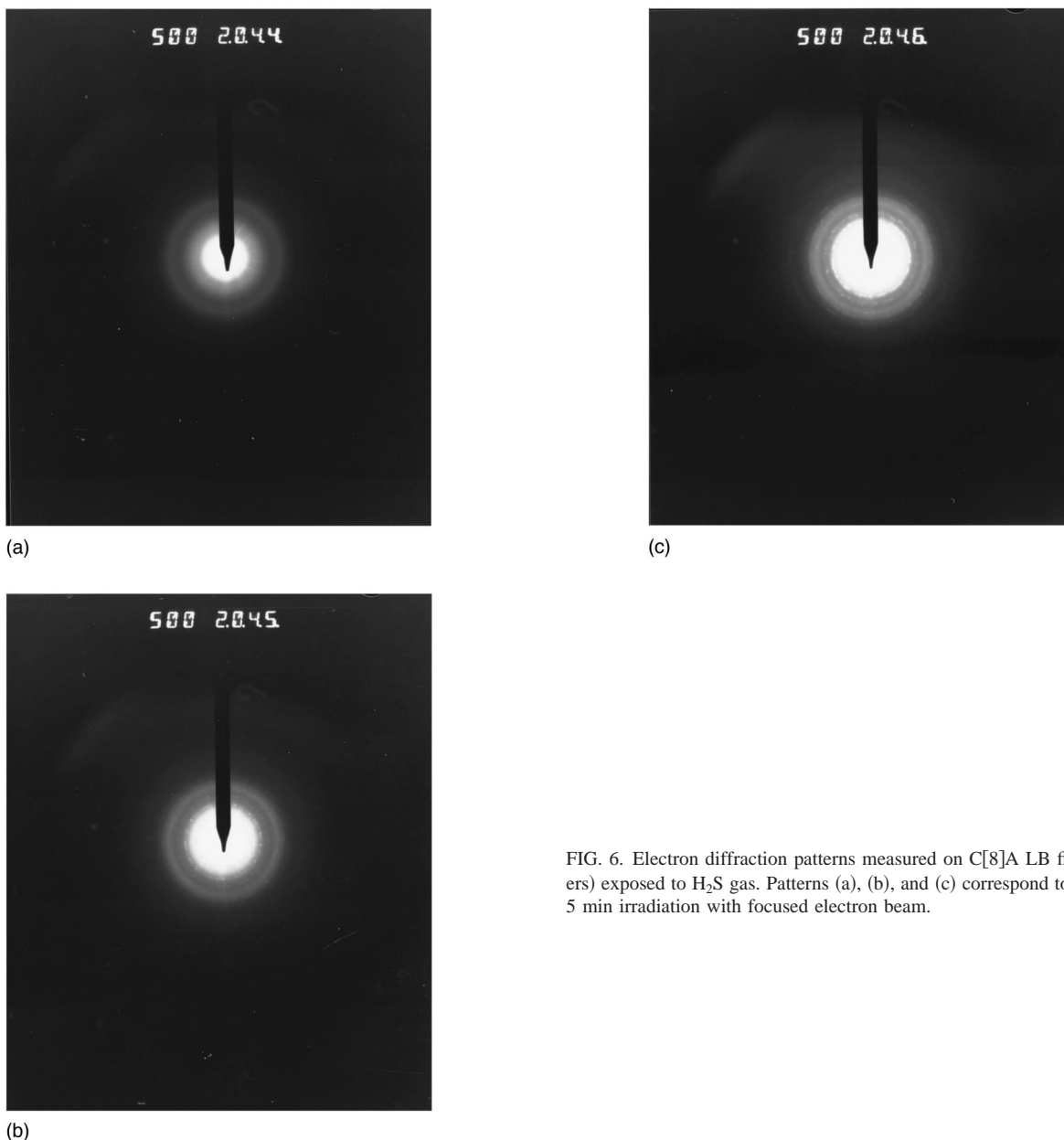
(a)

(c)

(b)

FIG. 6. Electron diffraction patterns measured on C[8]A LB film (ten layers) exposed to H_2S gas. Patterns (a), (b), and (c) correspond to subsequent 5 min irradiation with focused electron beam.

observation from x-ray and AFM studies that both the film structure and morphology have not changed after H_2S treatment.[16,17]

Figure 4 shows a subsequent shift in the minimum of the SPR curves to higher angles of incidence for two and four LB overlayers of C[8]A molecules in respect to that for bare gold film. As seen from Fig. 4, the treatment of the samples in H_2S gas affects both the gold film and LB overlayers. The SPR curve for bare gold has undergone a small shift due to the formation of a monolayer of sulphur on the gold surface as a result of reaction with H_2S gas. It can be assumed that the gold surface covered with gas permeable calixarene LB films is affected by the same reaction. As shown by the inset to Fig. 4, the slope of the dependence $\theta_{min}(N)$ is larger after the treatment with H_2S than before the treatment. This indicates that H_2S also affects the calixarene LB film due to the probable formation of CdS particles.

Calixarene matrix and CdS clusters are both virtually transparent at 633 nm. In order to evaluate refractive index n and film thickness d simultaneously,[25] values of $n = 1.46$ and $d = 1.5$ nm per C[8]A monolayer, previously obtained from ellipsometric measurements,[16] were used as starting values for the theoretical fitting to SPR data. Since the C[8]A LB films before H_2S treatment were transparent at 633 nm, $k = 0$ was postulated as a first guess value for the extinction coefficient. The obtained optical parameters for bare gold film and LB overlayers both before and after exposure to H_2S gas are summarized in Table I. The increase of extinction coefficient after exposure to H_2S gas may indicate the presence of semiconducting 2D planes of CdS within an insulator matrix, in which surface plasmon polaritons are thought to be excited. Similar results have been obtained from in situ SPR measurements during CdS formation within cadmium arachidate LB films.[26]

Figure 5 shows two TEM images which were taken at time intervals of 5 min on the same place of specimen under

continuos exposure to the electron beam. The growth of particles in both size and number with increasing time of exposure to a focused electron beam is very apparent. The size of the particles varies from 7 to 15 nm, which is much higher than that evaluated from the absorption spectra of the samples unexposed to an electron beam. It should also be pointed out that no particles were observed in the fresh samples of CdS/C[8]A LB films during initial stages of TEM experiments. This is in contrast to our previous TEM observation of CdS particles in stearic acid LB films, which appeared without stimulation by the electron beam.[17]

A set of three electron diffraction patterns of CdS/C[8]A LB film, taken at time intervals of 5 min, is shown in Fig. 6. They illustrate the transition from diffused rings for the fresh sample [Fig. 6(a)], corresponding to an amorphous carbon substrate, to spotty rings [Fig. 6(b)]. The rings become increasingly pronounced with the time of exposure [Fig. 6(c)]. These transformations in the diffraction pattern are believed to be caused by the growth of CdS clusters.

Values of spacing $D = 0.226$, 0.16, and 0.133 nm were evaluated from the diffraction pattern in Fig. 6(c) by using Bragg's formula $2D \sin \varphi = n\lambda$. The lattice parameters a_0 can be calculated by comparison of the experimental D values with D_{hkl} spacing[27]

$$a_0 = D_{hkl} \sqrt{h^2 + k^2 l^2}, \qquad (5)$$

where h, k, and l are Miller's indices for fcc zinc blende type lattice.

The last two values of 0.16 and 0.133 nm of spacing correspond most likely to (222) and (331) directions, respectively, and yield $a_0 = 0.567 \pm 0.012$ nm. The lattice parameter is less than a value of 0.583 nm for bulk CdS, which was predicted by Ramakhrishna's theory.[21] The spacing of 0.226 nm is not close to any crystallographic direction in fcc CdS zinc blende lattice and may correspond to the forbidden (211) direction with $D_{hkl} = 0.237$ nm. However, the structure of small CdS clusters may be sufficiently disturbed by the presence of calixarene matrix, and some other crystallographic directions become available. Knowing the area of 3.0 nm^2 occupied by the C[8]A molecule from Π-A isotherm measurements[15] and the number of CdS molecules per C[8]A unit of 2.85, obtained with XPS,[15] one can estimate the initial average distance between CdS molecules in the LB monolayer as 1.025 nm. This value is much higher than the obtained spacing of 0.567 nm in CdS clusters indicating segregation of CdS caused by the electron beam.

IV. CONCLUSION REMARKS

The observed blueshift of the main exciton absorption band[15,16] can be interpreted in terms of the formation of either very small CdS nanoclusters with the size of about 1.5 nm or 2D CdS planes with a thickness of about 1.7 nm within each calixarene bilayer. The fact that CdS nanoparticles were not observed in our previous experiments with both x-ray diffraction and AFM[16,17] favors the second model. In the present study, SPR measurements of LB films of calixarene Cd–salt show a sufficient increase in the extinction coefficient after exposure to H$_2$S gas, which indicates the

presence of conductive (semiconductive) inclusions within the film. TEM and electron diffraction shows no CdS particles in fresh samples of CdS/C[8]A LB films, but they have appeared later under exposure to a focused electron beam. The segregation of 2D CdS planes and formation of CdS nanoparticles stimulated by the electron beam is the most likely mechanism of the observed behavior.

Therefore, we succeed with the formation of two kind CdS nanostructures: 2D CdS planes initially formed within calixarene LB films, which can be later transformed to nanoclusters due to exposure to the high energy electron beam. This opens the direction for further research work toward the development of novel nanoelectronic and optoelectronic devices. In the case of 1.5 nm II–VI semiconductor clusters, switching elements can be fabricated on the basis of single-electron transistors[3,4] with well resolved at room temperature staircase-like current–voltage (I–V) characteristics. In contrast, superlattices consisting of 2D semiconducting plates may show electro-optical effect[28] or some other nonlinear optical properties. Moreover, Little's type high-temperature superconductivity[29] is expected for a single 2D semiconductor plane between two thin polar insulating layers. Further experiments are being undertaken to investigate mechanisms of planar conductivity and single-electron transfer across the films.

[1] F. Capasso, K. Mohammed, and A. Y. Cho, IEEE J. Quantum Electron. **QE-2**, 1853 (1986).

[2] M. Fukuda, N. Nakagava, S. Miyazaki, and M. Hirose, Appl. Phys. Lett. **70**, 2291 (1997).

[3] E. S. Snow, P. M. Campbell, R. W. Rendell, F. A. Buot, D. Park, C. R. K. Marian, and R. Magno, Semicond. Sci. Technol. **13**, A75 (1998).

[4] H. Weller, Angew. Chem. Int. Ed. Engl. **37**, 1658 (1998).

[5] J. H. Fendler and F. C. Meldrum, Adv. Mater. **7**, 607 (1995).

[6] N. A. Kotov, F. C. Meldrum, C. Wu, and J. H. Fendler, Phys. Chem. **99**, 2735 (1994).

[7] Yu. M. Lvov and G. Decher, Crystallogr. Rep. **39**, 628 (1994).

[8] N. A. Kotov, I. Dekany, and J. H. Fendler, J. Phys. Chem. **99**, 13065 (1995).

[9] A. Rauadel-Teixier, J. Leloup, and A. Barraud, Mol. Cryst. Liq. Cryst. **134**, 695 (1986).

[10] H. Weller, H. M. Schmidt, and U. Koch, Chem. Phys. Lett. **152**, 265 (1988).

[11] E. S. Smotkin, C. Lee, A. J. Bard, A. Campion, M. A. Fox, T. E. Mallouk, S. E. Webber, and J. M. White, Chem. Phys. Lett. **152**, 265 (1988).

[12] J. Leloup, A. Ruadel-Teixier, and A. Barraud, Thin Solid Films **210/211**, 407 (1992).

[13] X. G. Peng, R. Lu, Y. Y. Zhao, L. H. Qu, H. Y. Chen, and T. J. Li, J. Phys. Chem. **98**, 359 (1994).

[14] S. Ogava, F. R. F. Fan, and A. Bard, J. Phys. Chem. **99**, 11182 (1995).

[15] A. V. Nabok, T. Richardson, F. Davis, and C. J. M. Stirling, Langmuir **13**, 3198 (1997).

[16] A. V. Nabok, T. Richardson, C. McCartney, N. Cowlam, F. Davis, C. J. M. Stirling, A. K. Ray, V. Gassem, and A. Gibaud, Thin Solid Films **327–329**, 510 (1998).

[17] A. V. Nabok, A. K. Ray, A. K. Hassan, J. M. Titchmarsh, F. Davis, T. Richardson, A. Starovoitov, and S. Bayliss, Mater. Sci. Eng., C **8–9**, 171 (1999).

[18] A. K. Ray, A. K. Hassan, M. R. Saatchi, and M. J. Cook, Philos. Mag. **76**, 961 (1997).

[19] A. V. Nabok, A. K. Hassan, A. K. Ray, O. Omar, and V. I. Kalchenko, Sens. Actuators B **45**, 115 (1997).

[20] A. D. Yoffe, Adv. Phys. **42**, 173 (1993).

[21] M. V. Ramakhrishna and R. A. Frisher, J. Chem. Phys. **95**, 8309 (1991).

[22] L. E. Brus, J. Chem. Phys. **90**, 2555 (1986).

[23] Y. Kayanuma, Phys. Rev. B **38**, 9797 (1988).

[24] S. D. Smith, *Optoelectronic Devices* (Prentice Hall, Englewood Cliffs, NJ, 1995), p. 67.

[25] H. E. de Bruijn, B. S. F. Altenberg, R. P. H. Kooyman, and J. Greve, Opt. Commun. **82**, 425 (1991).

[26] N. J. Geddes, R. S. Urquhart, D. N. Furlong, C. R. Lawrence, K. Tanaka, and Y. Okahata, J. Phys. Chem. **97**, 13767 (1993).

[27] W. F. DeJong, *General Crystallography* (W. H. Freemam & Co, San Francisco, CA, 1959), p. 149.

[28] C. Weisbuch and B. Vinter, *Quantum Semiconductor Structures* (Academic, New York, 1991), p. 252.

[29] W. A. Little, in *Novel Superconductivity*, edited by S. A. Wolf and V. Z. Kresin (Plenum, New York, 1987), p. 341.